Printing Zn electrodes for a self-powered conductivity sensor

Author: Maria Dolors Grau Esteve
Facultat de Física, Universitat de Barcelona, Diagonal 645, 08028 Barcelona, Spain.

Advisors: Juan Marcos Fernández-Pradas (UB), Susana Liébana (IMB-CNM) and Neus Sabaté (IMB-CNM)

Abstract: A comparative study of screen-printing (SP) and Laser-Induced Forward Transfer (LIFT) techniques is conducted. Through both methods, SP inks are used to print Zn-based electrodes for a self-powered conductivity sensor. The optimal printing conditions of these inks via LIFT have been successfully determined. The printed electrodes performed quasi-indistinctively under electrochemical inspection, only differing in the effects created by the greater roughness of the LIFT printed electrodes.

I. INTRODUCTION

Point-of-care (PoC) devices are employed for medical testing outside a laboratory. By bringing the testing closer to the patient, rapid diagnosis results can be obtained so that an effective treatment can be promptly implemented. PoC testing has given rise to self-administered tests, allowing patients to evaluate their own health without the need of medical assistance. The increase in self-testing has led to the use of digital and single-use tests, where the whole device - usually composed of battery, sensor and electronics - is disposed after the health assessment, generating a large amount of waste.

For this reason, the Self-Powered Engineered Devices (SPEED) Research Group (IMB-CNM) developed and patented a paper-based battery as a conductivity sensor, where the power and sensing units are merged and the sample to be tested acts as the battery electrolyte, which significantly improves the sustainability of these devices. [1] This battery-sensor was made up of a Magnesium (Mg) anode and a Silver/Silver Chloride (Ag/AgCl) cathode, placed side-by-side, and covered with the paper used to absorb the sample. Though Mg performed properly, issues arose due to its high reactivity, as its sensing function was inconsistent for some electrolytes.

Therefore, Zn has been proposed as an alternative for the anode. [2] The choice of implementing a Zn-based anode was also made to adopt printable inks, so as to facilitate the production and improve the reproducibility of these batteries. Printing electronics [3] is a more sustainable and cost-effective method for fabricating electronics compared to traditional silicon-based production methods. While this technology offers many advantages, it presents one main limitation: the functional inks used for printed electronics are more resistive than the bulk materials.

One of the most utilized printing methods for printed electronics is screen-printing (SP), as it is remarkably cost-effective for large-scale production runs. SP is a printing technique that uses a mesh to transfer ink onto a substrate. The screen is permeable to ink in the image area (mesh), and non-permeable in the non-image area (emulsion). When the ink is pushed through the screen with a squeegee, the desired pattern is then printed onto the substrate. This working principle enables the use of inks with the highest solid content, thus performing closer to the bulk materials. As this method relies on the use of screens and stencils that must be developed for every new design, it becomes unsuitable for short production runs.[3]

On the other hand, direct-write printing techniques are typically digital techniques that arose from the formerly expressed need to print electronics in a customizable way. [4] They are particularly fitting for short-run printing, as they do not require the use of a master template. The most prominent direct-write printing technique is inkjet printing. However, the inks compatible with this technique carry low solid contents, which compromises the performance of the printed devices.

Laser-Induced Forward Transfer (LIFT) is a nozzle-free method for direct-write printing that uses a laser beam to transfer an amount of material from a donor layer onto a receiving substrate. It has been demonstrated that SP inks can be successfully printed using LIFT. [5] [6] A donor layer is extended on the donor substrate. Then, the laser beam is focused on the interface between the donor substrate and the donor layer. The laser pulse, that lasts some nanoseconds, creates a bubble in the donor layer, that when collapsing, generates a jet that is ejected forward towards the receiver, that is separated from the donor. This mechanism not only allows for many inks to be printed, but also to print on controlled areas with high precision on digital demand. Figure 1 shows a diagram of the operation of the SP and LIFT printing techniques.

In this work, SP inks are employed to produce the anode of the novel self-powered conductivity sensor developed by the SPEED Research Group. The electrodes are printed as a model with SP and LIFT methods, with the aim of evaluating the impact of the printing method on the performance of the sensor.

II. MATERIALS AND METHODS

A. Materials

The electrodes structure and geometry was designed by the SPEED Research Group. A scheme of the design can be seen in Figure 2. The materials used for the printing of the electrodes are: Polyethylene terephthalate (PET) substrate ($\approx$ 100 μm, Policrom Screens), silver (Ag)

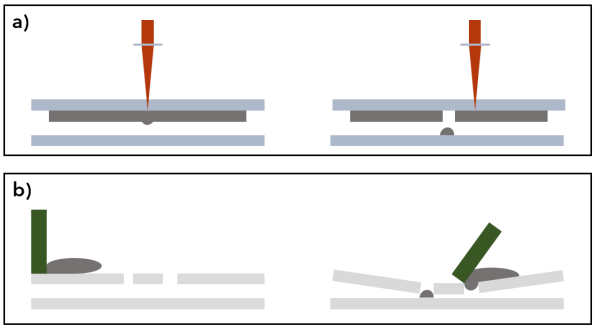

FIG. 1: Diagram depicting the mechanisms of ink deposition in the LIFT (a) and SP (b) methods.

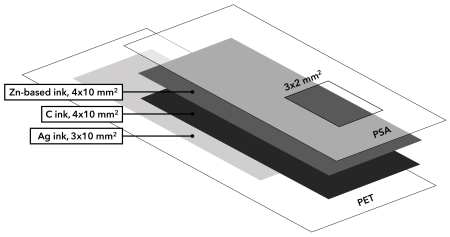

FIG. 2: Scheme depicting the design of the electrodes.

ink ECI 1010 (LOCTITE), carbon (C) ink C2030519P4 (SunChemical) and a 50 % mixture (in weigh) of the C ink and the Zn-based ink Saral Zinc 700 (Saralon), the mix was stirred manually for 1 hour to ensure the proper homogenization of the emulsion.

B. Screen-printing

The electrode fabrication process began with the pre-curing of the PET substrate at 130 $°C$ for 15 minutes. Then, the collector track was printed with the Ag ink and cured at 120 $°C$ for 15 minutes. Subsequently, a C ink layer was printed over the track to promote electron transfer, and cured at 60 $°C$ for 30 minutes. Finally, the working electrode was printed with the Zn-based ink mix, and cured at 80 $°C$ for 15 minutes.

C. Laser-Induced Forward Transfer

Laser system. A diode-pumped ytterbium fiber laser (Rofin PowerLine F20 Varia) was used. The laser works at the fundamental wavelength (1064 nm) with a pulse width ranging from 4 to 100 ns. The beam has a Gaussian intensity profile with output energies ranging from 2 to 775 μJ. The laser system has a galvanometric set of mirrors that allow the scanning of the sample at speeds ranging from 10 to 5000 mm/s. The repetition rate was maintained at 2000 Hz throughout the experiments. These parameters are regulated with the VisualLaserMarker software (Rofin), where the pattern to be printed is also defined.

Sample preparation. The donor layer was prepared using the doctor blade technique. Different donor layer thicknesses were employed during the experiments, ranging from 50 to 150 μm. For the receiver, the PET substrate was affixed to a microscope slide to ensure its flatness. In order to find the best printing conditions, different gap distances were tested, which were established through the use of varied combinations of 50 μm tape and 25 μm Kapton film.

D. Electrochemical Characterization

Voltammetry is an electrochemical technique used to study the behavior of a chemical species by measuring the current resulting from an applied potential. This response gives us information of the kinetic and thermodynamic aspects of the electron transfer processes. [7]

Experimental setup. A three-electrode cell is usually utilized to conduct voltammetric measurements. This cell consists of a working electrode (WE), a reference electrode (RE) and a counter electrode (CE), all submerged in the electrolyte. The electrochemical reaction of interest occurs at the working electrode. The reference electrode maintains a constant and known potential against which the potential of the working electrode is measured. The counter electrode completes the circuit, as it balances the current passing through the cell, maintaining charge neutrality.

The potentiostat is the instrument that applies a potential between the working and reference electrodes and measures the resulting current flowing through the cell.

The electrodes used for the voltammetry experiments were a platinum counter electrode (6.0351.100, Metrohm) and a Ag/AgCl reference electrode (6.0726.100, Metrohm). The macroscopic active area of the tested working electrodes was delimited with Pressure Sensitive Adhesives (PSA), as shown in Figure 2, leaving a working area of 6 mm^2. The cyclic voltammetry measurements were performed with the EmStat4 potenstiostat controlled by the PSTrace software (PalmSens). The linear sweep voltammetry experiments were conducted with the Autolab PGSTAT204 potentiostat controlled by the NOVA software (Metrohm).

Cyclic voltammetry (CV) is a type of potentiodynamic technique. In a CV experiment the working electrode potential is ramped linearly over time while observing the fate of the generated current. The potential is ramped from an initial potential value to a final one (forward scan), at a constant scan rate. Once the final potential is reached the potential is ramped in the opposite direction to the starting potential (reverse scan). [7]

In this work, CV is used to study the electron transfer mechanisms of a reversible redox reaction. In particular, the ferrocyanide/ferricyanide redox couple is used to detect the impact of the printing method on the performance and reproducibility of the electrodes.

An electrolyte composed of 5 mM of potassium hexacyanoferrate (II) trihydrate (Merk_P3289, 98.5 – 102 %, Sigma Aldrich) in a sodium chloride 100 mM solution (Merk_S9888, 99 %, Sigma Aldrich) is employed. Before the CV measurements the electrodes are activated applying a potential of 1.5 V for 20 sec.

In the cyclic voltammogram the anodic and cathodic peaks are observed, with a shape similar to the ones seen in Figure 3. The position and intensity of these peaks

are affected by the mechanisms of electron transfer at the electrode interface.

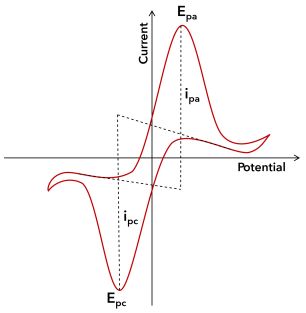

FIG. 3: Scheme of the cyclic voltammetry of the ferrocyanide/ferricyanide redox couple.

At 25 $^{\circ}C$, the peak current is described by the Randles-Sevcik equation:

$$i_p = 2,69 \cdot 10^5 \cdot n^{3/2} \cdot A \cdot C \cdot D^{1/2} \cdot v^{1/2}$$

where:

i_p = peak current (A), n = number of electrons exchanged per molecule, A = electroactive area of the electrode (cm^2), C = concentration of analyte (mol/cm^3), D = difusion coefficient (cm^2/s), v = potential scan rate (V/s).

The experimental determination of the peak current, allows one to calculate the parameters appearing in the expression. The ratio between the current of the cathodic and anodic peaks, i_{pc}/i_{pa}, is the parameter that allows us to judge the chemical reversibility of the redox reaction. For an ideal reversible electrochemical reaction this ratio is 1. Another parameter that indicates electrochemical reversibility is the peak-to-peak separation, ΔE_p is a constant equal to 59 mV for ideal one-electron transfer electrochemical reactions at 25 $^{\circ}C$.

Linear Sweep Voltammetry (LSV) is also a potentiodynamic technique. In this method the current at the working electrode is measured while the potential is swept linearly in time. The current signal begins to appear at the potential which the species begins to oxidize or reduce.

In this work the oxidation of the printed Zn-based electrodes is studied, in order to evaluate their performance and consistency.

The electrochemical reaction taking place at the Zn electrode is:

$\mathrm{Zn(s)} \longrightarrow \mathrm{Zn^{2+}(aq)} + 2\,\mathrm{e^-}$

With this technique the open circuit potential and the current-potential curve are registered.

E. Electrode Morphology Characterization

The morphology of the laser printed samples was studied through an optical microscope (Carl Zeiss, AXIO Imager.A1). Then, an optical microscope (Canon,) and a confocal microscope (Sensofar, PLμ 2300) were used for the electrode surface characterization.

III. RESULTS

A. LIFT Printing

To achieve a successful printing of the electrodes using SP inks, the laser printing parameters must be optimized. Our main goal was to attain controlled and reproducible surface printing using LIFT. To accomplish this one must determine the conditions under which single pixels are adequately printed. When the desired conditions are found the line printing conditions can also be determined, before determining the ones for surface printing.

Several parameters influence droplet deposition: laser pulse amplitude and energy, donor thickness and gap distance. Each ink has its unique rheological behavior, thus this parameters have to be especially determined. For every ink we experimented with different donor thicknesses and gap distances, for which we printed series of pixels with pulse amplitudes of 4, 8, 14 and 20 ns with energies ranging from 135.5 ± 0.5 to 2.5 ± 0.5 μJ.

First, we studied the printing conditions of the Ag ink on a PET substrate. The donor thickness and gap distance that ensured better results were of 50 μm and 75 μm, respectively. The minimum energy required to deposit droplets is 9.9 ± 0.5 μJ. Over this energy two distinct behaviors are observed: for the lower energies, until 16.0 ± 0.5 μJ, pixels of diameters ranging from 100 to 150 ± 10 μm are printed. For higher energies the diameters range from 570 to 720 ± 10 μm. This can be explained as follows: at the lowest energies the bubble does not reach the receiver, springing back to the donor layer. At intermediate energies the droplet is deposited through jets. For higher energies the droplet is deposited through the contact of the bubble with the receiver substrate. [5]

Thereafter, the same study was conducted for the carbon ink on glass and silver substrates. The preferred donor thickness and gap were 50 μm and 50 μm, respectively. For both substrates the threshold printing energy was identical, 6.6 ± 0.5 μJ. The diameter range of the pixels was also similar, spanning from 40 to 540 ± 10 μm. The behavior of the diameter with respect to the pulse energy changes for the different substrates. On glass, the relationship is clearly quadratic, whereas on silver the behavior is logarithmic, see Figure 4. This is not the only difference, as on silver, the droplets printed with energies higher than 49.0 ± 0.5 μJ, are deposited with splash and satellites, as the high energy causes the bubbles to burst.

Finally, this same test were performed for the Zn-based and C ink mixture. The lumps and agglomerations that form in the Zn ink create a challenge for ensuring the homogeneity of the donor layer. For this reason, this layer needed to be 150 μm thick. The gap was kept at 50 μm. The threshold energy for this ink is of 9.5 ± 0.5 μJ, above which the droplets have diameters ranging from 300 ± 10 to 610 ± 10 μm. A linear but scattered relationship between the energy pulse and the pixel diameter can be sensed.

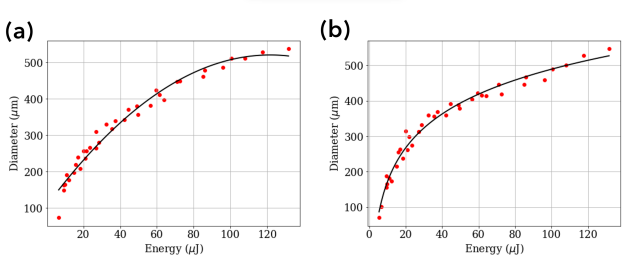

FIG. 4: Plots showing the diameter of the deposited pixels at different pulse energies. (a) C ink on glass, with a second degree polynomial fit (b) C ink on Ag ink, with logarithmic fit.

In accordance with our goal of printing electrodes, adequate droplet printing conditions need to be established for every ink. The droplets have to be stable and of regular shape. Therefore the pulse amplitude and energy with which lines are printed is: For the Ag ink, 8 ns and 35.5 ± 0.5 μJ, with pixel diameters of 600 ± 10 μm; for the C ink 4 ns and 27.0 ± 0.5 μJ, with pixel diameters of 300 ± 10 μm; and for the Zn and C ink mix, 14 ns at 108.0 ± 0.5 μJ, with pixel diameters of 700 ± 10 μm. Lines are created by overlapping pixels, that is placing the centers of such pixels at distances shorter than their diameter. For each ink, lines with varying overlaps were printed. The results are presented in Figure 5. The overlap at which an ink is considered to be properly printed is the one where scalloping is minimized and no clumping or discontinuities appear. For the Ag ink the overlap at which this conditions are met is of the 80 %, for the C ink of the 40 %, and for the Zn and C ink mix it is also of the 40 %.

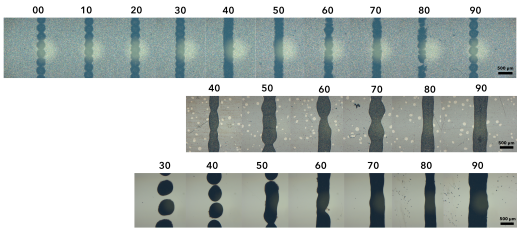

FIG. 5: Optical images showing (from top to bottom) lines of C on a Ag ink substrate, Ag ink on PET and Zn and C ink mix on glass. The scale bar represents 500 μm

The printing of surfaces is accomplished by placing lines adjacently. The distance between the pixel centers that form a line and the ones of the neighboring line is called spacing. The silver tracks were printed with a spacing of 200 μm, for the carbon layer it was set at 300 μm and for the Zn and C layer it was 460 μm.

B. Electrochemical Characterization

In this section comparative study of the electrochemical performance of SP and LIFT printed electrodes is conducted.

Figure 6 shows the cyclic voltammograms of different carbon electrodes. From this measurements the electroactive area of the eletrodes can be estimated. As well as the effect of the printing method on the reversibility of the electrochemical reaction. Table I includes the parameters obtained from the CV analysis. The changes in the performance of the electrodes are subtle, but relevant. Firstly, one can see how the electroactive area of the LIFT printed electrodes is larger than the one of the SP ones. This is due to the greater roughness of this electrodes. [10] Secondly, it can be seen how the reversibility of the redox reactions in a cell containing SP electrodes is higher. A flatter surface can allow simpler difusion and mass transport mechanisms, favouring the reversibility. [8]

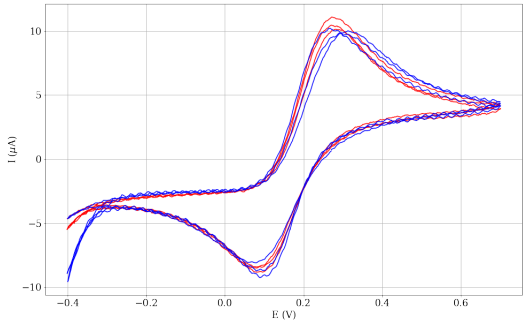

FIG. 6: Triplicates of CV of potassium hexacyanoferrate(II) 5 mM in 100 mM of soldium chloride salt solution with carbon electrodes printed by SP (blue) and LIFT (red). The data corresponds to the second scan, performed with a scan rate of 0.01 V/s. The potential is measured $vs.$ the Ag/AgCl.

TABLE I: Values obtained from the CV analysis. These are the averaged parameters of the triplicates.

	Screen	**Laser**
$I_{pa}(\mu A)$	12.9 ± 0.1	13.5 ± 0.3
$E_{pa}(V)$	0.28 ± 0.01	0.28 ± 0.06
$I_{pc}(\mu A)$	-10.9 ± 1.0	-9.6 ± 0.9
$E_{pc}(V)$	0.095 ± 0.006	0.090 ± 0.007
$A(mm^2)$	3.70 ± 0.04	3.87 ± 0.08
I_{pa}/I_{pc}	1.2 ± 0.1	1.4 ± 0.1
$\Delta E_p(V)$	0.184 ± 0.006	0.184 ± 0.006

Figure 7 displays the averaged LSV curves. From this evaluation one can obtain the OCP of the cell as well as the slope at the pre-peak region. These values are shown in Table II. The theoretical value of the OCP of pure Zn corresponds to its standard electrode potential, -0.761 V (cite) $vs.$ SHE [11], or -0.958 V $vs.$ Ag/AgCl [7], which is compatible with the experimental value found in this work. Both SP and LIFT printed electrodes' OCP differs from the ideal value, as the surface is composed of a mix of C and Zn-based inks, having LIFT printed electrodes a value slightly closer to the ideal one.

The slope of the LSV curve in the pre-peak region, can provide information about the rate of the electrochemical

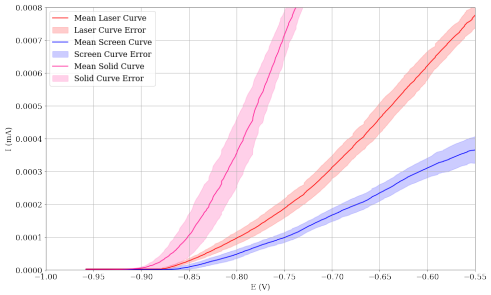

FIG. 7: Linear sweep voltammetry of the Zn printed electrodes and Zn solid foil in sodium chloride 100 mM. The scan rate is of 0.01 V/s. The curves are the averaged value of n=5 repeats.

TABLE II: Parameters obtained from the averaged LSV curves, n=5. OCP *vs.* Ag/AgCl.

	OCP (V)	**Slope** $(1/\Omega)$
Solid	-0.946 ± 0.007	$(7.25 \pm 0.02) \cdot 10^{-3}$
Screen	-0.863 ± 0.007	$(1.31 \pm 0.01) \cdot 10^{-3}$
Laser	-0.881 ± 0.006	$(2.97 \pm 0.01) \cdot 10^{-3}$

reaction or the sensitivity of the system to changes in potential. These are influenced by diffusion effects, species adsorption and other complex mechanisms, which are at the same time determined by the electrode's surface. As it can be seen in Figure 8, the LIFT electrodes have a rugged surface, whereas the surface of the SP electrodes is much flatter. Accordingly, it has already been seen that LIFT printed electrodes have a greater electroactive area, which may be the cause of the greater amount of current generated at a given potential compared to the SP electrodes.

IV. CONCLUSIONS

In this work a comparative study of printed Zn-based anodes through SP and LIFT was conducted. We were able to determine the optimal printing parameters of the SP inks for LIFT.

The LIFT printed electrodes exhibited a furrowed surface compared to the relatively flat surface of the SP electrodes. This difference has potentially enhanced the electrochemical behavior of the LIFT electrodes, as seen

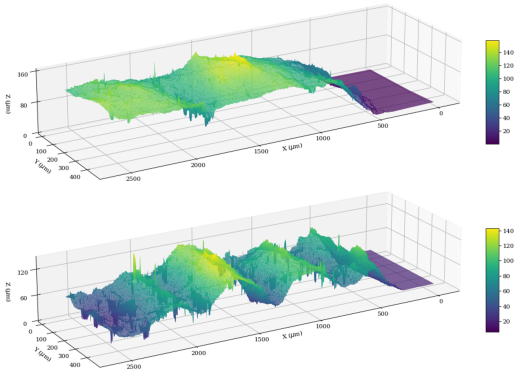

FIG. 8: Relief of the electrode surfaces. Top: SP. Bottom: LIFT.

in the LSV analysis, backed by the greater electroactive area obtained via CV. However, through CV it has also been found that SP electrodes yeild an environment that favours the reversibility of the redox reaction.

SP is a well established method for the large-scale production of printed electronics. LIFT with a proven capacity of printing SP inks, can serve as a substitute for SP during prototyping stages, especially when a digital printing technique is required. Furthermore, it can be used to explore the effects of roughness on the electrochemical behavior of electrodes.

Acknowledgments

I would like to express my deepest gratitude to my advisors, Juan Marcos Fernández-Pradas and Susana Liébana, for their continuous support and guidance. I am grateful for the opportunity they provided me. Special thanks also to Ernest Martí and Aida Visús, their help and insights were fundamental for the development of this work.

[1] Ortega, L., Lorella, A., Esquivel, J.P., Sabaté, N. (2020). Paper-Based Batteries as Conductivity Sensors for Single-Use Applications. ACS Sensors.
[2] Juan, O. (2023). Zn-AgCl paper-based battery as ionic conductivity sensor. Treballs Finals de Grau - Física UB.
[3] Wu, W. (2022). Printed Electronics Technologies. Royal Society of Chemistry.
[4] Fernández-Pradas, J.M., Serra, P. (2020). Laser-Induced Forward Transfer: A Method for Printing Functional Inks. Crystals.
[5] Sopeña, P., Fernández-Pradas, J.M., Serra, P. (2020). Laser-induced forward transfer of conductive screen-printing inks. Applied Surface Science.
[6] Sopeña, P., Sieiro, J., Fernández-Pradas, J.M., Lopez Villegas, J.M., Serra, P. (2020). Laser-Induced Forward Transfer: A Digital Approach for Printing Devices on Regular Paper. Advanced Materials Technologies.
[7] Zanello, P. (2003). Inorganic electrochemistry: Theory, practice and aplication. Royal Society of Chemistry.
[8] Kant, R. (2010). General Theory of Arbitrary Potential Sweep Methods on an Arbitrary Topography Electrode and Its Application to Random Surface Roughness. The Journal of Physical Chemistry C.
[9] Menshykau, D. Streeter, I., Compton, R.G. (2008). Influence of Electrode Roughness on Cyclic Voltammetry. The Journal of Physical Chemistry C.
[10] Dhillon, S., Kant, R. (2013). Quantitative roughness characterization and 3D reconstruction of electrode surface using cyclic voltammetry and SEM image. Applied Surface Science.
[11] Vanýsek, P. (2012). "Electrochemical Series". CRC Handbook of Chemistry and Physics (93rd ed.). pp. 5–80.